HNUE JOURNAL OF SCIENCE DOI: 10.18173/2354-1075.2021-0230
Educational Sciences, 2021, Volume 66, Issue 5A, pp. 198-206
This paper is available online at http://stdb.hnue.edu.vn

A THEORETICAL STUDY OF THE CRYSTAL STRUCTURES AND ELECTRONIC PROPERTIES OF BULK MoS_2 AND ITS MONOLAYER BASED ON FIRST – PRINCIPLES CALCULATION

Doan Thi Kieu Anh[1], Tran Phan Thuy Linh[2,*] and Luong Viet Mui[3]
[1]*Institute of Physics, Vietnam Academy of Science and Technology*
[2]*Department of Physics, Hanoi National University of Education*
[3]*Graduate School of Engineering, Osaka University, Japan*

Abstract. In this work, we have investigated the structural and electronic properties of both bulk and monolayer MoS_2 based on the density functional theory (DFT) implemented in the CASTEP of Materials Studio package. The calculations are performed with the local density approximation (LDA) and generalized gradient approximation (GGA) functionals for crystal structure optimization and band structure of MoS_2 bulk and monolayer. Our calculations show that the GGA functional calculated excellent band gap for bulk MoS_2, while LDA functional is found to perform better for band gap calculations of a monolayer. The influence of composition in the energy bands has been realized by analyzing the partial density of states (PDOS) of each atom and density of states (DOS). By reducing the layer thickness from bulk to monolayer, it is found that band structure has the transitions from indirect band gap in the bulk MoS_2 (1.53 eV) to direct band gap in the monolayer (1.82 eV). On the other hand, the charge density difference along z-direction shows that the major charge transfer occurs on the surface of the S atoms and there is a little accumulation around the surface of the Mo atoms. This property highlights the promising of MoS_2 in improving the fabrication of optoelectronic devices in the future.

Keywords: MoS_2 bulk and monolayer, bandgap, energy band structure, optoelectronic device.

1. Introduction

Graphene possesses many properties such as the linear dispersion with energy near the Dirac point [1], high electron mobility at room temperature [2], and high thermal conductivity of 5000 $Wm^{-1}K^{-1}$ [3, 4], so it has attracted heightened attention because of their potential applications in energy storage, solar cell, transparent electrodes, etc. However, graphene is not a semiconductor (or insulator) since the conduction band and valence band is symmetrical about Dirac point, that making the zero-gap spectrum in graphene. The unusual properties of graphene are limited for a variety of novel applications. Recently, researchers have been focusing on other 2D materials. The rapid progress in the methodology of preparing ultrathin layers has brought about the exploration of layer transition metal dichalcogenides (LTMDs) with similar structures to graphene.

Transition metal dichalcogenides (TMDs) materials are a new class of two-dimensional (2D) which is defined as transition metal and chalcogenides of MX_2 type (M = Mo, W, Ti, Zr, Hf, V,

Received October 11, 2021. Revised November 4, 2021. Accepted December 5, 2021.
Contact Tran Phan Thuy Linh, e-mail address: linhtpt@hnue.edu.vn

Nb, Ta, Tc, Re, Co, Rh, Ir, Ni, Pd, Pt and X = S, Se, Te). TMDs materials have unusual crystal structure because their electronic characters could be semiconducting, metallic, or superconducting [5]. They have been attracting a wide range of research interests due to variety of applications in flexible band gap which can change from bulk to monolayer, easy to fabricate complex structures out of them, energy storage or make a positive contribution to the markets of nanoscale electronics and spintronic devices.

Molybdenum disulfide (MoS_2) is a representative member of the transition metal dichalcogenide family of materials. MoS_2 has been one of the most studied transition metal dichalcogenides because they are widespread as molybdenite. It has attracted lots of interest because of its outstanding properties such as unusual optical property, robust mechanical property, oxidative resistance and superior electrical performance which make it scientific, and industrial importance [6]. MoS_2 has been the subject of significant research in many fields including photovoltaics, photocatalysis for energy conversion, nanoelectronics, energy storage in nonaqueous lithium batteries, electrochemical hydrogen storage, switching device, capacitors, sensing, catalytic hydride sulfurization of petroleum and hydrogen evolution reaction, solid lubricant for wear resistance, intercalation host, bioelectronics and biology [7-11]. MoS_2 is constructed of three atom layers (Mo^{4+} layer is sandwiched between two S^{2-} layers by covalent bonds in a sequence of S – Mo – S) stacked together through weak Van der Waals interaction [12, 13]. Unlike graphene with the band gap is zero, bulk MoS_2 is semiconducting with an indirect bandgap of 1.2 eV, whereas single-layer MoS_2 is a direct gap semiconductor with a bandgap of 1.8 eV [14, 15]. The strong emission due to the direct gap structure of monolayer MoS_2 is used in optoelectronics [16] and field-effect transistors (FETs) [17]. More recent technology has drawn for bulk MoS_2 is to use in photocatalytic [18] and photovoltaic [19] materials.

Therefore, in this review, to clear up the structural and electronic properties of MoS_2 in bulk and its monolayer, we performed a study using a planar wave Norm conserving pseudopotential technique based on first-principles density functional theory with different exchange correlation functional. The rest of this content is organized as follows. The computational method that we used in this work is shown in Section 2.1. Section 2.2, we briefly describe the results and discussion. Firstly, the structure crystal of bulk MoS_2 is described. Then, the electronic properties using LDA and GGA calculations are displayed. Section 3 we give a short summarizes our findings and outlook for future research on MoS_2.

2. Content

2.1. Computational methods

In this work, we performed the first-principles density functional theory (DFT) calculations implemented in the CASTEP (Cambridge Serial Total Energy Package) module of Materials Studio (MS). We have used norm-conserving, local density approximation (LDA) in Ceperlay Alder (CA) compare with Perdew - Burke - Ernzerhof (PBE) of the generalized gradient approximation (GGA) as the exchange correlation. From the convergence test, the cutoff energy and the k reciprocal lattice points for our calculation are 510 eV and 5x5x1, respectively.

By using the CASTEP module, we performed the lattice relaxation computation for both MoS_2 bulk and monolayer in order to obtain lattice constants *a* and *c* and the total energy minimization with respect to unit cell volume. By editing lattice planes with Miller indices (0 0 1), monolayer MoS_2 was created and visualized with VESTA software. After that, these structures were used for further calculations such as electronic band structure and density of states and of bulk and monolayer MoS_2. For both bulk and monolayer MoS_2, the electronic band structures were performed with the high symmetry points using the G-M-K-G-K-path. All of the results also compared to the available experimental and previous calculation.

2.2. Results and discussion

2.2.1. Structural parameters

Figure 1 presents the crystal structure of bulk MoS_2. Structurally, MoS_2 can be considered a kind of a hexagonal system which belong to the $P6_3/mmc$ space group. Figure 2 shows the 4x4 supercell from top and side views. As shown in two Figures, the MoS_2 unit cells have structure as sandwiches with two S layers and one Mo layer. Each Mo atom has six S nearest neighbors located in the top and bottom S-S layers. In bulk MoS_2 has two S-Mo-S layers while monolayer MoS_2 has a single such layer.

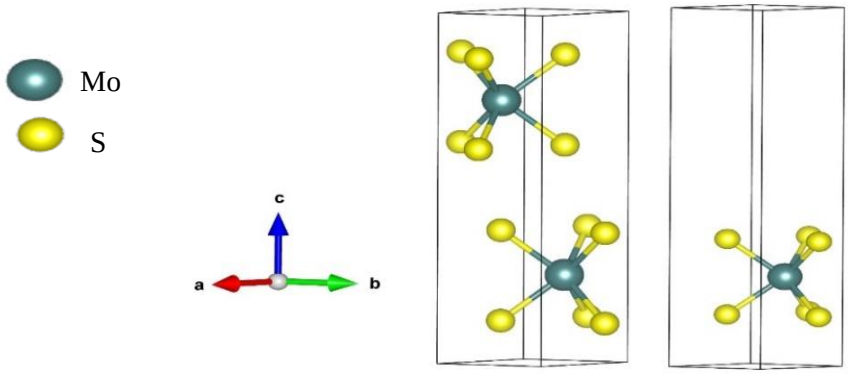

Figure 1. Crystal structure of bulk and monolayer MoS_2

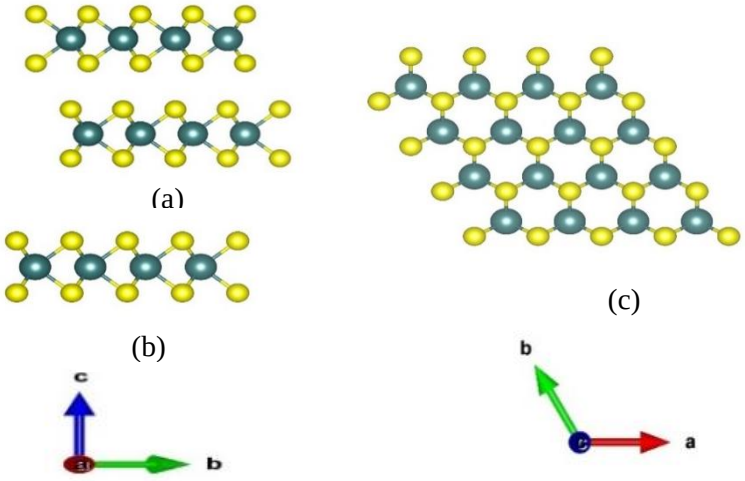

Figure 2. (a) (b) Side view of bulk and monolayer MoS_2; (c) Top view of bulk and monolayer MoS_2

With the lattice relaxation computation and using both LDA and GGA as the exchange-correlation functional, the parameters of the electronic structure such as lattice constants, bond lengths for bulk, and monolayer MoS_2 are determined as presented in Table 1. It is clear that the relaxed lattice parameters calculated for bulk MoS_2 are the same as those of monolayer MoS_2 and nearly equal when compared to the experimental and other previous reports. In particular, it emphasizes that our calculations related to the structural parameters for bulk MoS_2 are very close to those of monolayer when using local density approximations functional.

Table 1. Structural parameters of bulk MoS_2 and monolayer MoS_2 using LDA and GGA

Properties	Bulk MoS_2				Monolayer MoS_2		
	Present calculation		*Previous reports*	*Experiment [22]*	*Present calculation*		*Previous reports*
	LDA	*GGA*			*LDA*	*GGA*	
Lattice constant a=b (Å)	3.17	3.21	3.19 [20], 3.17 [23]	3.16	3.16	3.20	3.20 [24] 3.23 [20]
c/a ratio (Å)	3.87	4.76	3.86 [20]	3.89	3.87	4.75	-
Bond length (Mo – S) (Å)	2.42	2.44	2.45 [21]	2.41	2.42	2.44	2.45 [21] 2.42 [24]
Distance (S-S) (Å)	3.17	3.21	3.12 [21] 3.18 [21]	3.19	3.17	3.21	3.13 [21] 3.18 [21]

2.2.2. Band structures

For a detailed comparison between bulk and monolayer MoS_2, we calculated the band structure using the exchange-correlation LDA and GGA with the k reciprocal lattice points 5×5×1 for the Brillouin zone and the cutoff energy is 510 eV. The calculation results are presented in Table 2.

Table 2. Band gap energy for bulk MoS_2 and monolayer MoS_2 using both LDA and GGA

Function	Bulk MoS_2	Monolayer MoS_2
LDA + CA-PZ	0.81	1.82
GGA + PBE	1.53	1.67

There is a significant difference in band gap values calculated by using LDA and GGA for bulk and monolayer of MoS_2. By using the LDA, we obtained bulk MoS_2 is a semiconductor with narrow indirect band gaps of 0.81 eV, while this result is 1.53 eV when GGA is used. Unlike the origin bulk MoS_2, for monolayer MoS_2, the band gap is a direct band gap with the value of 1.82 eV or 1.67 eV when LDA or GGA is applied, respectively. It is important to have a more accurate energy band gap of materials, especially for the semiconductor. To be more specific about the results, our calculated band gaps for bulk and monolayer MoS_2 are compared with the experimental and theoretical band gaps and shown in Table 3. For the LDA functional, it is seen that the indirect band gap of bulk MoS_2 has value of 0.81 eV, which is smaller than the experiment a value of 1.29 eV [26] by 37.2% and 1.23 eV [27] by 34.1%. On the other hand, monolayer MoS_2 has a value smaller than the experiment by 1.11%. Compared with the GGA functional, we obtained the band gap value for bulk smaller than its experiment value by 18.6%, while monolayer MoS_2 has band gap value of 1.67 eV smaller than 7.22%. Thus, by comparing the values with the experimental data, we see that the LDA functional is found to perform better for band gap calculations of the monolayer, while GGA functional calculated band gap for bulk MoS_2 is quite good agreement with previous reports. The main reason can come from the unusual crystal structure of bulk and monolayer MoS_2.

Table 3. Calculated band gap using LDA function and compare with some reference

	Bulk MoS_2		**Monolayer MoS_2**	
	Result	*Reference*	*Result*	*Reference*
Band gap (eV)	0.81	Previous calculation	1.82	Previous calculation
		0.89 [20], 0.75 [23], 1.06 [25]		1.57[20], 1.2 [23], 1.71 [28]
		Experiment		Experiment
		1.29 [26], 1.23 [27]		1.8 [14]
Band gap Characteristic	Indirect		Direct	

2.2.3. Density of states

Figure 3 shows the electronic band structure of bulk MoS_2 corresponding to the density of states (DOS). The results show that bulk MoS_2 is indirect - gap semiconductor that have a band edge located at the G point and the midpoint between K and G points. For monolayer the top of the valence band and the bottom of the conduction band are both originate at high - symmetric K point, performing the direct band gap semiconductor as can be seen in Figure 4.

In particular, the difference of band gap between bulk and monolayer MoS_2 is more clearly as can be seen in Figure 3 and 4. We observed that the band edge of bulk MoS_2 is smaller than its monolayer. Hence, there is a transition from indirect band gap of bulk MoS_2 to direct band gap of monolayer MoS_2. It is worth mentioning here that the DOS of bulk is almost double that its monolayer. Simply because of the structure of MoS_2: In bulk MoS_2 has two S-Mo-S layers while monolayer MoS_2 has a single such layer. This indicates our calculated structure may be more feasible.

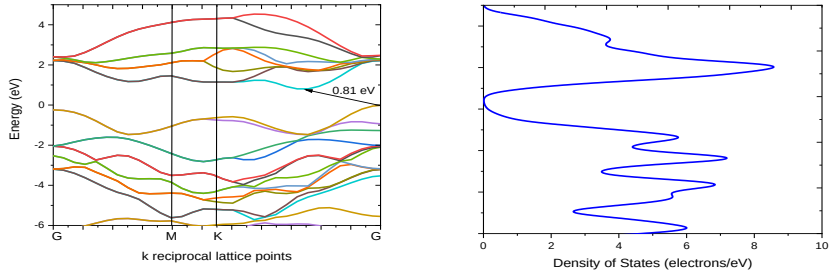

Figure 3. Band structure and Density of States of Bulk MoS_2 with LDA functional

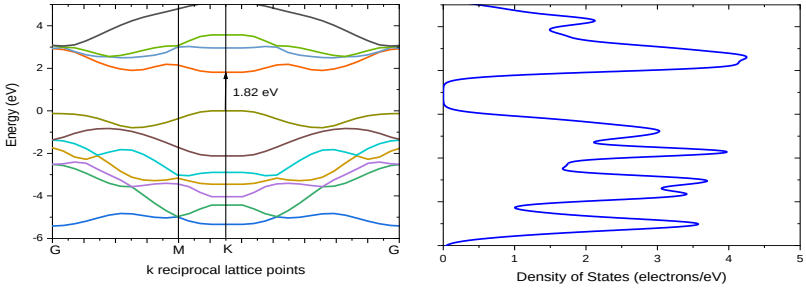

Figure 4. Band structure and Density of States of Monolayer MoS_2 with LDA functional

2.2.4. Partial density of states

We calculated the partial density of states (PDOS) of each atom in bulk MoS_2 and compared it to its monolayer and presented in Figure 5. Our PDOS shows that the d states of metal ion (Mo) and the p states of sulfur atoms strongly hybridized the top of the valence band - bottom of the

conduction band. Besides, it is seen that the f states of both atoms Mo and S disappear in these edges of bulk and monolayer. The energy bands around the Fermi energy originate mainly from the Mo- d states. On each side of the band gap are derived mainly from 4d states of Mo and 3p states of S. The results agree perfectly with previous reports.

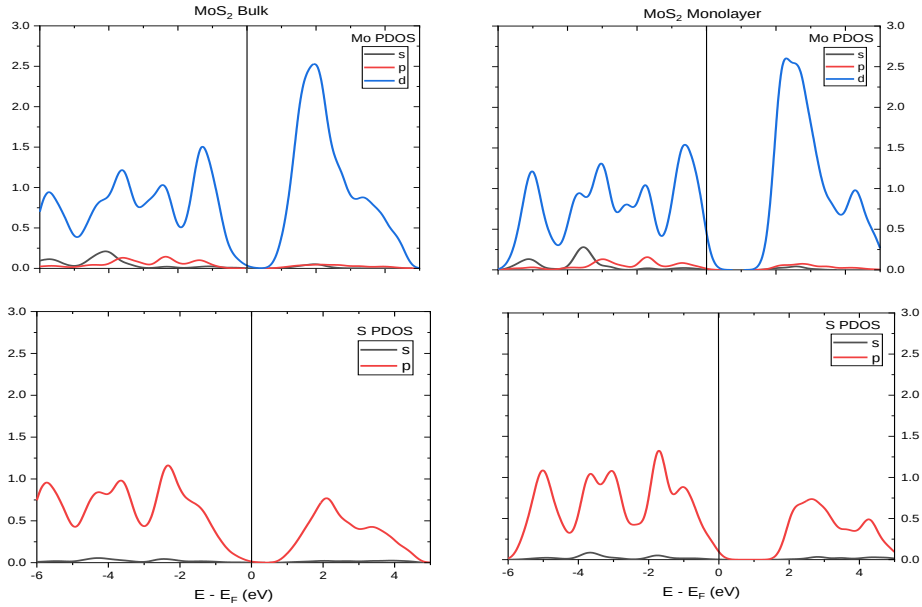

Figure 5. Partial Density of States of Mo and S atoms for Bulk and Monolayer MoS_2 using LDA functional

2.2.5. Electronic charge density

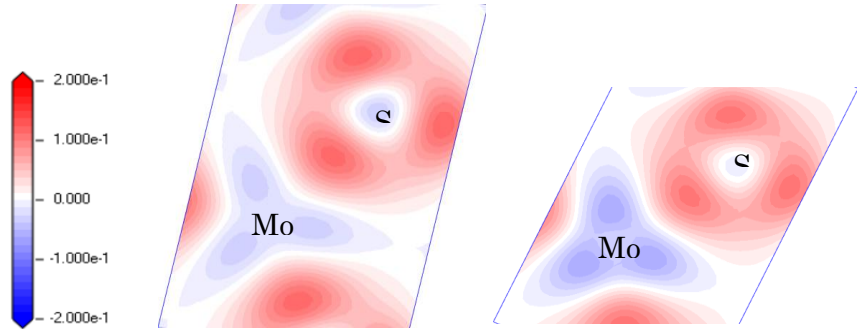

Monolayer MoS_2 Bulk MoS_2

Figure 6. The electron charge density of (0 0 1) surface for both bulk and monolayer MoS_2

Figure 6 shows (001) the surface of the charge density difference along the z-direction, where the red regions represent a gain of charge while the blue denote a loss of charge. It is clear that the major charge transfer occurs on the surface of the S atoms and there is a little accumulation around the surface of the Mo atoms. As a result, the electronic charge sharing between the atoms, as found in polar covalent bonds, suggests a stronger interaction between Mo and S atoms [29, 30]. The results are the same in both bulk and monolayer MoS_2 and are in good with previous reports. In other words, the repulsive forces between S atom surfaces are larger than the repulsive forces of Mo - atom surfaces. This makes the MoS_2 can be used for electric applications which improve the charge-discharge rate of the batteries.

3. Conclusions

In summary, we investigated the structural and electronic properties of MoS_2 using the density functional theory implemented in CASTEP of the Material Studios Package. The Perdew Burke Ernzerhof (PBE) formalism was employed with generalized gradient approximation (GGA) compared with the local density approximation (LDA). The electronic structures and properties of bulk and monolayer MoS_2 were calculated. It is found that bulk MoS_2 is a semiconductor with narrow indirect band gaps of 1.53 eV for the transitions from Q to the midpoint between K and Q, whereas monolayer MoS_2 has a direct band gap is 1.82 eV at high - symmetric K point. The GGA functional calculated excellent band gap for bulk MoS_2, while LDA functional is found to perform better for band gap calculations of the monolayer. This is highlight indirect - direct band gap transition for MoS_2. Not only that, a strong hybridization between metal d and chalcogen p states below the Fermi energy was found from the partial density of states of each atom. It is also found that states around Fermi energy are mainly due to the metal d states. Our observation is consistent with the theoretical prediction of indirect to direct band gap transition for bulk MoS_2 to its monolayer. On the other hand, the charge density difference along z-direction shows that the major charge transfer occurs on the surface of the S atoms and there is a little accumulation around the surface of the Mo atoms. The result indicated the electronic charge sharing between the atoms, as found in polar covalent bonds, suggesting a stronger interaction between Mo and S atoms. This makes the MoS_2 can be used for electric applications which improve the charge-discharge rate of the batteries.

REFERENCES

[1] Charlier, J.-C., Eklund, P. C., Zhu, J., & Ferrari, A. C., 2007. Electron and Phonon Properties of Graphene: Their Relationship with Carbon Nanotubes. *Carbon Nanotubes*, pp. 673-709.

[2] K.S Novoselov, A.K. Geim, S.V. Morozow, D. Jiang, S.V. Dubonos, I.V. Grigorieva, and A.A. Firsov, 2004. Electric Field Effect in Atomically Thin Carbon Films. *Science*, 306(5696), pp. 666-669.

[3] Ghosh, S., Calizo, I., Teweldebrhan, D., Pokatilov, E. P., Nika, D. L., Balandin, A. A., … Lau, C. N., 2008. Extremely high thermal conductivity of graphene: Prospects for thermal management applications in nanoelectronic circuits. *Applied Physics Letters*, 92(15), 151911.

[4] Chen, S., Wu, Q., Mishra, C., Kang, J., Zhang, H., Cho, K., … Ruoff, R. S., 2012. Thermal conductivity of isotopically modified graphene. *Nature Materials*, 11(3), pp. 203-207.

[5] A. K. Geim, I. V. Grigorieva, 2013. Van der Waals heterostructures. *Nat.* Vol. 499, pp. 419-425.

[6] N. Goswami, A. Giri, S. K. Pal, 2013. MoS_2 nanocrystals are confined in a DNA matrix exhibiting energy transfer. *Langmuir*, Vol. 29, pp. 11471-11478.

[7] S. Z. Butler, S. M. Hollen, L. Cao, Y. Cui, J. A. Gupta, H. R. Gutierrez, T. F. Heinz, S. S. Hong, J. Huang, A. F. Ismach, E. Johnston-Halperin, M. Kuno, V. V. Plashnitsa, R. D. Robinson, R. S. Ruoff, S. Salahuddin, J. Shan, L. Shi, M. G. Spencer, M. Terrones, W. Windl, J. E. Goldberger, 2013. Progress, challenges, and opportunities in two-dimensional materials beyond graphene. *ACS Nano*, Vol. 7, pp. 2898-2926.

[8] J. S. Ross, S. Wu, H. Yu, N. J. Ghimire, A. M. Jones, G. Aivazian, J. Yan, D. G. Mandrus, D. Xiao, W. Yao, X. Xu, 2013. Electrical control of neutral and charged excitons in a monolayer semiconductor. *Nat. Commun.*, Vol. 4, pp. 1-6.

[9] M. Chhowalla, H. S. Shin, G. Eda, L.-J. Li, K. P. Loh, H. Zhang, 2013. The chemistry of two-dimensional layered transition metal dichalcogenide nanosheets. *Nat. Chem.*, Vol. 5, pp. 263-275.

[10] S. Ding, D. Zhang, J. S. Chen, X. W. D. Lou, 2012. Facile synthesis of hierarchical MoS_2 microspheres composed of few-layered nanosheets and their lithium storage properties. *Nanoscale*, Vol. 4, pp. 95-98.

[11] S. Wi, H. Kim, M. Chen, H. Nam, L. J. Guo, E. Meyhofer, X. Liang, 2014. Enhancement of photovoltaic response in multilayer MoS_2 induced by plasma doping. *ACS Nano*, Vol. 8, pp. 5270-5281.

[12] X. Wang, F. Nan, J. Zhao, T. Yang, T. Ge, K. Jiao, 2015. A label-free ultrasensitive electrochemical DNA sensor based on thin-layer MoS_2 nanosheets with high electrochemical activity. *Biosens. Bioelectron*, Vol. 64, pp. 386-391.

[13] D. Jariwala, V. K. Sangwan, L. J. Lauhon, T. J. Marks, M. C. Hersam, 2014. Emerging device applications for semiconducting two-dimensional transition metal dichalcogenides. *ACS Nano*, Vol. 8, pp. 1102-1120.

[14] K. F. Mak, C. Lee, J. Hone, J. Shan, T. F. Heinz, 2010. Atomically thin MoS_2: A new direct-gap semiconductor. *Phys. Rev. Lett.*, Vol. 105, pp. 1-4.

[15] A. Splendiani, L. Sun, Y. Zhang, T. Li, J. Kim, C.-Y. Chim, G. Galli, F. Wang, 2010. Emerging photoluminescence in monolayer MoS_2. *Nano Lett.*, Vol. 10, pp. 1271-1275.

[16] W. Wu, L. Wang, Y. Li, F. Zhang, L. Lin, S. Niu, D. Chenet, X. Zhang, Y. Hao, T. F. Heinz, J. Hone, Z. L. Wang, 2014. Piezoelectricity of single-atomic-layer MoS_2 for energy conversion and piezotronics. Nat., Vol. 514, pp. 470-474.

[17] X. Li, H. Zhu, 2015. Two-dimensional MoS_2: Properties, preparation, and applications. J. Mater., Vol. 1, pp. 33-44.

[18] Fortin, E., & Sears, W. M., 1982. Photovoltaic effect and optical absorption in MoS_2. *Journal of Physics and Chemistry of Solids*, 43(9), pp. 881-884.

[19] Gourmelon, E., Lignier, O., Hadouda, H., Couturier, G., Bernède, J. C., Tedd, J., Salardenne, J., 1997. MS_2 (M = W, Mo) photosensitive thin films for solar cells. *Solar Energy Materials and Solar Cells*, 46(2), pp. 115-121.

[20] Ahmad, S. and Mukherjee, 2014. A Comparative Study of Electronic Properties of Bulk MoS_2 and Its Monolayer Using DFT Technique: Application of Mechanical Strain on MoS_2 Monolayer. S. *Graphene*, 3, pp. 52-59.

[21] Kumar, A., & Ahluwalia, P. K., 2012. A first principle comparative study of electronic and optical properties of 1H - MoS_2 and 2H - MoS_2. *Materials Chemistry and Physics*, 135(2-3), pp. 755-761.

[22] Wilson, J. A., & Yoffe, A. D., 1969. The transition metal dichalcogenides discussion and interpretation of the observed optical, electrical and structural properties. *Advances in Physics*, 18(73), pp. 193-335.

[23] Kuc, A., Zibouche, N., & Heine, T., 2011. Influence of quantum confinement on the electronic structure of the transition metal sulfideTS_2. *Physical Review B*, 83(24).

[24] Ataca, C., Şahin, H., Aktürk, E., & Ciraci, S., 2011. Mechanical and Electronic Properties of MoS_2 Nanoribbons and Their Defects. *The Journal of Physical Chemistry C*, 115(10), pp. 3934-3941.

[25] Ramakrishna Matte, H. S. S., Gomathi, A., Manna, A. K., Late, D. J., Datta, R., Pati, S. K., & Rao, C. N. R., 2010. MoS_2 and WS_2 Analogues of Graphene. *Angewandte Chemie International Edition*, 49(24), pp. 4059-4062.

[26] Dolui, K., Pemmaraju, C. D., & Sanvito, S., 2012. Electric Field Effects on Armchair MoS_2 Nanoribbons. *ACS Nano*, 6(6), pp. 4823-4834.

[27] Kam, K. K., & Parkinson, B. A., 1982. Detailed photocurrent spectroscopy of the semiconducting group VIB transition metal dichalcogenides. *The Journal of Physical Chemistry*, 86(4), pp. 463-467.

[28] Yazyev, O. V., & Kis, A., 2015. MoS_2 and semiconductors in the flatland. *Materials Today*, 18(1), pp. 20-30.

[29] Li, H., Yu, K., Li, C., Tang, Z., Guo, B., Lei, X., … Zhu, Z., 2015. Charge-Transfer Induced High Efficient Hydrogen Evolution of MoS_2/graphene Cocatalyst. *Scientific Reports*, 5(1).

[30] Aray, Y., Vega, D., Rodriguez, J., Vidal, A. B., & Coll, D. S., 2009. Atoms in molecules theory for exploring the crystal structure and bond nature of the MoS_2 bulk. *Journal of Computational Methods in Sciences and Engineering*, 9(4-6), pp. 257-267.